Colloid Polym Sci (2011) 289:247–255
DOI 10.1007/s00396-010-2342-3

ORIGINAL CONTRIBUTION

Dynamic rheology studies of in situ polymerization process of polyacrylamide–cellulose nanocrystal composite hydrogels

Chengjun Zhou · Qinglin Wu · Quanguo Zhang

Received: 13 September 2010 / Revised: 1 November 2010 / Accepted: 12 November 2010 / Published online: 4 December 2010

Abstract A series of dynamic small-amplitude oscillatory shear experiments for in situ polymerization process of polyacrylamide–cellulose nanocrystal (PAM–CNC) nanocomposite hydrogels were performed to investigate the relationship between rheological properties and synthesis parameters including chemical cross-linker concentration, polymerization temperature, initiator concentration, and CNC aspect ratios. The results showed that CNCs accelerated the onset of gelation (t_{onset}) and acted as a multifunctional cross-linker during the gelation reaction. The composite hydrogels exhibited enhanced steady-state elastic modulus $\left(G'_{\infty}\right)$ and plateau loss factor ($tan\delta$) compared to these of the pure PAM hydrogels, indicating that adding CNCs not only reinforced but also toughened PAM hydrogels. $\left(G'_{\infty}\right)$ and the effective network junction density (N) increased with increased cross-linker concentration, polymerization temperature, and CNC aspect ratios, but decreased with increased initiator concentration. The changes of plateau $tan\delta$ were opposite to that of G'_{∞}. The sol–gel transition kinetics of PAM–CNC hydrogels accelerated with increased cross-linker concentration and polymerization temperature and, however, reached optimization at 0.25 wt% of initiator concentration. CNCs with lower aspect ratios promoted t_{onset} and the sol–gel transition of PAM–CNC hydrogels, suggesting the fact that CNCs with lower aspect ratios further facilitated the formation of network of PAM–CNC nanocomposite hydrogels.

Keywords Polyacrylamide · Cellulose nanocrystals · Nanocomposite hydrogels · Dynamic rheology · In situ polymerization

C. Zhou · Q. Wu (✉)
School of Renewable Natural Resources,
Louisiana State University Agricultural Center,
Baton Rouge, LA 70803, USA
e-mail: wuqing@lsu.edu

Q. Zhang
Energy Engineering Laboratory, Henan Agricultural University,
Zhengzhou 450002, China

Introduction

The nanocomposite polymer hydrogels (NPHs), defined as cross-linked polymer networks swollen with water in the presence of nanoparticles or nanostructures, are new generation materials that can be used in a wide variety of applications including stimuli-responsive, microfluidics, catalysis, separation, pharmaceutical, and biomedical devices [1]. NPHs, in comparison with conventional hydrogels, can provide improved mechanical strength and ability for remote controlling [2]. Currently, the most commonly available matrix for nanocomposite hydrogels are polyacrylamide (PAM) and its derivatives due to their nontoxic and biological inertness, long chain length, capacity for preserving their shape and mechanical strength, and convenient adjustability of mechanical, chemical, and biophysical properties [3, 4]. For the past decade, a large number of researches have been conducted to improve mechanical and chemical properties of hydrogels with adding nanofillers into polyacrylamide-based matrix. These nanofillers include polymer nanoparticles [5–7], inorganic clay [8, 9], and metal nanoparticles [10]. However, little effort has been made to fabricate NPHs with natural biopolymer nanofillers originated from renewable natural recourses. In our recent work, cellulose nanocrystals (CNCs) were successfully incorporated into PAM hydrogels by in situ polymerization, and it was found that the

biopolymer nanofillers effectively enhanced the mechanical properties of hydrogels [11].

Although a possible mechanism for forming hydrogels was proposed based on the investigation into the chemical structure, morphology, swelling and compression properties, and gelation process of this hydrogels with different CNC concentration [11], it is highly desirable to investigate the kinetics of in situ polymerization reactions in order to better understand the cure and formation mechanisms of macroscopic gelation for these novel NPHs. Furthermore, it is also valuable for controlling and optimizing the gelation process and functional performance of NPHs. A variety of experimental techniques have been employed to study the gelation kinetics of PAM-based hydrogels. Among these techniques, dynamic rheology has emerged as an effective and powerful approach for gel characterization because in situ experiments are relatively facile to perform during the polymerization process, and viscoelastic properties could directly reflect the structure and morphology of hydrogels [12, 13]. Most importantly, dynamic tests can be used effectively to monitor cross-linking and microstructural changes in hydrogel systems without disrupting microstructure and kinetics of the sol–gel process through small amplitude oscillatory shear as a function of cross-linking time at a particular angular frequency. Generally, pure PAM gels were prepared by free-radical cross-linking copolymerization of acrylamide (AM) monomer and *N*,*N*′-methylenebisacrylamide (NMBA) cross-linker in the presence of a radical initiator. Calvet et al. [14] determined the gelation kinetics of PAM hydrogels by a series of in situ small-amplitude oscillatory shear experiments under various cross-linker concentrations and reaction temperatures, and found the optimal cross-linker concentration and temperature conditions for the maximum elasticity of hydrogels. Chiriac et al. [15, 16] studied the effects of heating rate, shear stress, and the weight ratio of redox initiators pair on the sol–gel transition for PAM gels by in situ dynamic rheology, and optimized polymerization conditions through elastic properties of the obtained hydrogel. These studies illustrate that dynamical rheology techniques are capable of distinguishing appropriate polymerization conditions for the fabrication of PAM hydrogels with desired properties.

Although great effort has been made on monitoring in situ polymerization of pure PAM hydrogels by the dynamic rheology, there are only a few reports concerning the PAM-based nanocomposite hydrogel. Okay and Oppermann [17] performed a rheology investigation on the gelation reactions of polyacrylamide–clay nanocomposite hydrogels with and without chemical cross-linker NMBA. The gelation process of nanocomposite hydrogels composed of sulfonated polyacrylamide and montmorillonite was also studied using oscillatory time sweeps [18].

In this study, gelation kinetics and rheological properties of polyacrylamide–cellulose nanocrystal (PAM–CNC) nanocomposite hydrogels during in situ polymerization process were studied by using dynamical oscillatory shear rheology technique. The nanocomposite hydrogels were prepared by polymerization of AM in the presence of CNCs with NMBA as a cross-linker using the redox initiation based on potassium persulfate/sodium bisulfate. Compared to the previous work, the preparation process of PAM–CNC hydrogels in the present work was redesigned to meet the dynamic rheology measurement. The objective was to elucidate the effects of synthesis parameters (including cross-linker concentration, polymerization temperature, initiator concentration, and aspect ratios of nanofillers) on structure–property relationships of nanocomposite hydrogels.

Experimental

Materials

CNCs were isolated from commercial microcrystalline cellulose by combined acid hydrolysis with 63% H_2SO_4 and high-pressure homogenization process as described in our previous work [19]. The nanocrystals homogenized for one and five cycles are designated as CNC1 and CNC5. The rod-shaped CN1 and CN5 had the average lengths of 113±25 and 62±26 nm, and average diameters of 8.5±1.8 and 8.7±1.2 nm, respectively. Thus, the aspect ratios of CNC1 and CNC5 were about 11 and 6, respectively. In addition, the zeta potential was −31.8 for CNC1 and −34.0 for CNC5 at the 0.5 wt% concentrations, respectively. AM and NMBA were purchased from Sigma-Aldrich Inc. (St. Louis, MO). Potassium persulfate (KPS) and sodium bisulfite (SBS) were purchased from Thermo Fisher Scientific Inc. (Fair Lawn, NJ) and EM Industries Inc. (Gibbstown, NJ), respectively. The above chemicals were used as received. The aqueous solutions in all experiments were prepared with distilled water.

Synthesis of PAM–CNC nanocomposite hydrogels

At a fixed 10 wt/vol.% of the total mass–volume concentration ($\%C_T$), PAM–CNC nanocomposite hydrogels were prepared by free-radical polymerization of AM in fresh CNC aqueous suspensions in the polymerization temperature range of 5–45 °C, cross-linker mass concentration ($\%C_{NMBA}$) range of 0.17–2 wt%, and initiator mass concentration ($\%C_{IN}$) range of 0.1–0.75 wt%. The term $\%C_T$ refers to the total mass of AM, CNCs, and cross-linker per unit volume of gel solution, while $\%C_{NMBA}$ and $\%C_{IN}$, respectively, refer to the percentages of cross-linker and

initiator KPS by weight of the total mass of AM, CNCs, and cross-linker, as shown in the following equations:

$$\%C_T = \frac{m_{AM} + m_{CNC} + m_{NMBA}(g)}{V_{sol}(ml)} \times 100 \quad (1)$$

$$\%C_{NMBA} = \frac{m_{NMBA}(g)}{m_{AM} + m_{CNC} + m_{NMBA}(g)} \times 100 \quad (2)$$

$$\%C_{IN} = \frac{m_{IN}(g)}{m_{AM} + m_{CNC} + m_{NMBA}(g)} \times 100 \quad (3)$$

where the mass ratio of monomer AM to CNCs is 95 to 5. In addition, the redox initiator is composed of KPS and SBS, and their mass ratio is 5 to 3 for KPS to SBS. The detailed synthesized conditions and sample names are shown in Table 1. The change of cross-linker concentration, temperature, initiator concentration, and CNC dimension for PAM–CNC systems are designated to NH, TH, IH, and CH, respectively.

The stock solutions of the cross-linker and the initiator system in distilled water were freshly prepared prior to each experiment. They were cooled in an ice-water bath to decrease the effect of temperature on the incubation period. To illustrate the synthesis procedure of composite hydrogels, the preparation of PAM–CNC–NH2 is described in detail as follows. A sample of 47 ml of 5.29×10^{-3} g ml^{-1} fresh CNC suspension was poured into a 100-ml dry flask with a magnetic force stirrer. Then, 4.7263 g of AM monomer was added to the suspension, and it was deoxygenated with bubbling nitrogen for 15 min in an ice-water bath. One milliliter of 2.5×10^{-2} g ml^{-1} NMBA cross-linkers, 1 ml of 1.25×10^{-2} g ml^{-1} KPS, and 1 ml 0.75×10^{-2} g ml^{-1} SBS fresh solution were continuously added to the mixture solution and mixed drastically under nitrogen atmosphere for 5 min. Thereafter, this solution was immediately loaded onto the lower plate of the rheometer for monitoring gelation process.

The pure polyacrylamide hydrogel without CNCs was synthesized according to the conventional method [8, 20], which is the same as these described above for PAM–CNC–NH2 hydrogel synthesis without addition of CNCs.

Rheology monitoring of gelation process

Rheology monitoring of gelation was performed using two parallel plates and oscillatory time sweep testing mode with an AR2000ex Rheometer (TA Instruments Inc., New Castle, DE). The upper plate was made of stainless steel with a 40-mm diameter. The lower plate was a Peltier device with a specially designed temperature control system. During measurement, a sample of 0.6 ml of the reactive solution was poured on the lower Peltier plate, and then, the upper plate was set at a distance of 500 μm above the Peltier plate. Low viscosity silicon oil was used to seal the gap between two plates for minimizing the evaporation during the rheology testing. An angular frequency of w= 1 rad s^{-1} and a deformation amplitude $r°$=0.01 were selected to ensure that the dynamic oscillatory deformation was within the linear regime.

The viscosity measurements of the 0.5×10^{-2}-g ml^{-1} CNC suspension with and without the redox initiator were also performed on the AR2000ex Rheometer. Viscosities were measured using a cone plate of 60 mm in diameter. The temperature of CNC suspension was controlled by the Peltier device at 25 °C, and the shear rate was fixed at 7.34 s^{-1}. To avoid the evaporation of water and the oxygen contamination, 58 μm of gap between cone and parallel plates was sealed with the solvent trap cover, and the moat on the top of the cover was filled with the low viscosity silicon oil.

Table 1 Synthesis conditions of PAM and PAM–CNC hydrogels

Sample name[a]	$\%C_{NMBA}$/wt%	$\%C_{IN}$/wt%	Temperature/°C	CNC type
PAM	0.50	0.25	25	–
NH1	0.17	0.25	25	CNC1
NH2	0.50	0.25	25	CNC1
NH3	1.00	0.25	25	CNC1
NH4	2.00	0.25	25	CNC1
TH1	0.50	0.25	5	CNC1
TH2	0.50	0.25	35	CNC1
TH3	0.50	0.25	45	CNC1
IH1	0.50	0.10	25	CNC1
IH2	0.50	0.75	25	CNC1
CH1	0.50	0.25	25	CNC5

[a] *NH*, *TH*, *IH*, and *CH* refer to the change of cross-linker concentration, temperature, initiator concentration, and *CNC* dimension, respectively

Results and discussion

Viscosity changes of CNC suspension with and without the redox initiator

The flow properties with retention time for CNC suspensions with and without initiator are illustrated in Fig. 1. It can be observed that the aqueous CNC1 suspension firstly showed an initial remarkable shear-thinning behavior with a large decrease of apparent viscosity at a 7.34-s^{-1} shear rate. The 0.5×10^{-2} g ml^{-1} of CNC suspension was the semi-dilute isotropic at-rest fluid, which forming particular physical network of CNCs suspended in water was disturbed and oriented with shear [21]. The viscosity then gradually decreased and reached an equilibrium value. After adding redox initiator into the CNC1 suspension, it also displayed the shear-thinning characteristic during the first 200 s, and then thickened gradually with retention time. This behavior was possibly because of the presence of uronic acid and sulfate groups on the CNC surface from the acid hydrolysis during CNC production [22, 23]. These groups were screened by the increased ionic strength for the addition of the K^+ and Na^+ of initiator, hindering the electrostatic repulsions between the CNCs but enhancing their interactions. Tandjawa et al. observed similar phenomena with their investigation of the viscoelastic behavior of defrosted cellulose microfibril suspensions by addition of salt [24]. In addition, the thickening behavior of CNC suspensions with the initiator also suggests that an initiator can interact with rigid-rod CNCs through ionic interactions and associated on the CNC surface in aqueous suspensions [25].

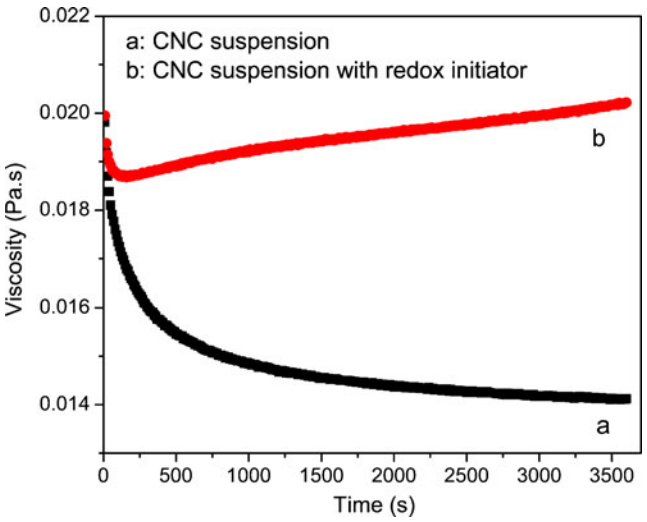

Fig. 1 Viscosity variations as a function of retention time for 0.5×10^{-2}-g ml^{-1} aqueous CNC1 suspensions without (**a**) and with (**b**) 2.5×10^{-4}-g ml^{-1} l redox initiator at the 7.34-s^{-1} shear rate

Gelation process of PAM and PAM–CNC hydrogels

The gelation process of gels was monitored by in situ dynamic small-amplitude oscillatory shear measurements using the time sweep mode at 1 rad s^{-1} of angular frequency and 1% of strain. The storage modulus (G') and loss factor ($tan\delta=G''/G'$, i.e., the ratio of dissipated energy to stored energy) as a function of time during the polymerization of pure PAM and PAM–CNC are shown in Fig. 2. In general, it can be seen that the gelation process of both systems can be divided into three periods. First, there was a short incubation period (stage I), in which the system behaved as a viscous liquid until the gelation point was reached (taken as the point where $tan\delta=1$). After the onset of gelation, G' increased rapidly within about half an hour (stage II), which was a sol–gel process for reaction system. During the final plateau period (stage III) of gelation process, G' slightly increased and reached the final equilibrium value. From Fig. 2, the onset of gelation (t_{onset}) of CNC-free and CNC-doped system calculated was 4.1±0.4 and 2.5±0.3 min, respectively. This result indicates that the

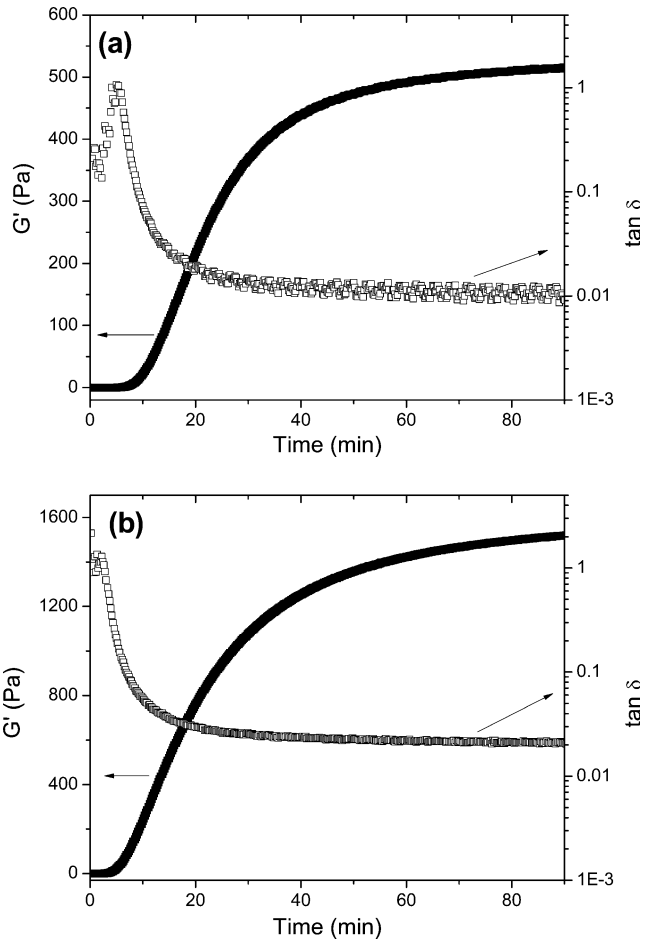

Fig. 2 Variations of elastic modulus G' and loss factor $tan\delta$ as a function of polymerization time for pure PAM (**a**) and PAM–CNC–NH2 nanocomposite (**b**) hydrogels

induction time of PAM hydrogels was decreased by the addition of CNCs because of the interference of the physical network of rod-shaped CNCs. Furthermore, this network can be improved after adding an initiator into polymerization system (as described above). Thus, the overlapped action of the physical network of CNCs with chemical network of PAM chain likely accelerated the onset of gelation. Due to the initiator attached on CNC surface in aqueous suspensions, free-radical polymerization of AM with the KPS/SBS redox system can be initiated on the surface of CNCs, which was consistent with our previous investigation [11]. Meanwhile, the other initiator existed in solution initiated the homopolymerization of AM to grow PAM macromolecule chains, which were cross-linked by the NMBA. Finally, the PAM network loaded with CNCs was formed. The possibly optimal network of PAM–CNC hydrogel is depicted in Fig. 3.

To estimate the final steady-state elastic modulus of the gels, G'_{∞} (Pa), the experimental data of G' time of stage II shown in Fig. 2a were fitted to a modified Hill equation [14]:

$$G'(t_{gel}) = G'_{\infty}\frac{{t_{gel}}^n}{{t_{gel}}^n + k^n} \quad (4)$$

Where, t_{gel} (minutes) is the gelation time (i.e., the total time minus the induction time), k (minutes) is the half-gelation time (i.e., $G'(k)=G'_{\infty}/2$), and n is a coefficient relative to the asymptotic slope P (Pa·min^{-1}) at the half-gelation time. P, calculated by the following equation, can be used to quantitatively characterize the sol–gel transition kinetics:

$$P = nG'_{\infty}/4k \quad (5)$$

Based on the curve fitting data, G'_{∞} for the CNC-free (i.e., pure PAM) and CNC-loaded hydrogel systems were 517±28 and 1567±94 Pa, respectively. Thus, the equilibrium G' of PAM–CNC hydrogels was almost threefold higher than that of pure PAM hydrogels. In addition, the values of P for CNC-free and CNC-loaded hydrogels were 27.4±1.5 and 41.4±2.5 Pa min^{-1}, respectively, indicating that the sol–gel transition kinetics of PAM hydrogels was accelerated by CNCs because the strong interactions between PAM chains and the nanocrystals restricted the mobility of the polymer chain. Thus, the presence of CNCs increased the entanglement density of PAM chain. Since shear elastic modulus G in the theory of rubber elasticity corresponds to the final steady-state elastic modulus G'_{∞} [17], the effective network junction density N (in mol·m^{-3}) in hydrogels related to the G'_{∞} can then be expressed as [14, 26]:

$$G'_{\infty} = \mathrm{NRT} \quad (6)$$

where R and T are the gas constant (8.314 JK^{-1} mol^{-1}) and absolute temperature (K), respectively. The estimated N values for PAM and PAM–CNC hydrogels were 0.21±0.012 and 0.63±0.038 mol m^{-3}, respectively, suggesting that CNCs acted as a multifunctional cross-linker in addition to a reinforce agent. The plateau values of loss factor ($tan\delta$) were 0.01±0.001 for pure PAM and 0.02±0.003 for PAM–CNC, respectively, as shown in Fig. 2b. Such small values of $tan\delta$ (i.e., G' was two orders of magnitude higher than G'') for hydrogels with and without CNCs during the final polymerization process present that they are strong gels with negligible viscous properties. It is worth noting that the plateau $tan\delta$ of PAM–CNC hydrogels slightly increased compared to that of pure PAM, indicating that the viscous properties increased faster than the elastic properties. This behavior is beneficial to the improved toughness of hydrogels based on the energy dissipation mechanism [27].

Effect of cross-linker concentration for PAM–CNC hydrogels

In order to investigate the influence of cross-linker concentration, a series of experiments were performed on PAM–

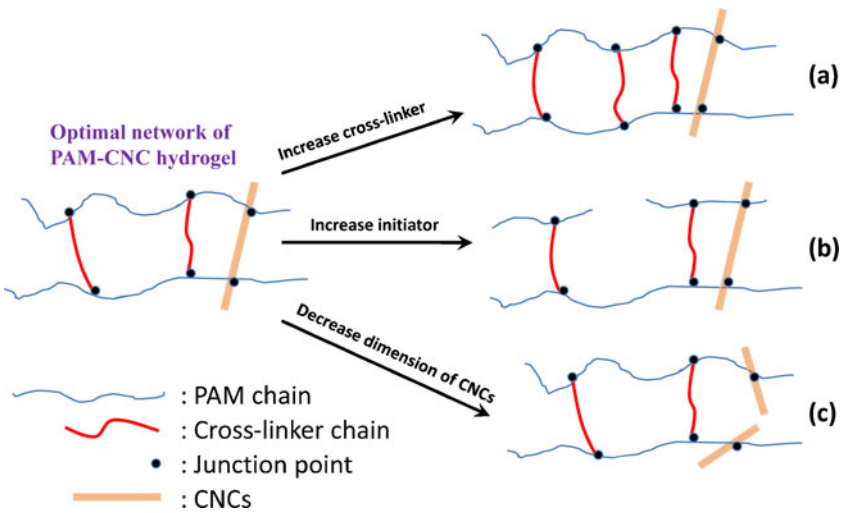

Fig. 3 Scheme of the effect of cross-linker (**a**), initiator (**b**), and CNC dimension (**c**) on network microstructure of PAM–CNC hydrogels

CNC compositions of 10 $\%C_T$ with cross-linker concentrations ranging from 0.17 to 2 wt%. The G'_∞ and *tanδ* for PAM–CNC nanocomposite hydrogels with different cross-linker concentrations as a function of time during the polymerization are shown in Fig. 4. The G'_∞ and P increased and t_{onset} decreased with increased cross-linker concentration over the entire range of compositions studied, which indicates that cross-linker NMBA enhanced the capability to form effective network junction for PAM–CNC hydrogel system. This behavior was further shown by the increase in the effective network junction density N with increase of cross-linker concentration, similar to the previous results about the effect of cross-linkers NMBA on pure PAM hydrogel [13, 14, 28]. This increase in junction density was in turn accompanied by a decrease in the average molecular weight of polymer strands linking two neighboring junctions (Fig. 3a), suggesting that the gel network was interconnected with a shorter molecular chain. It should be noted that the plateau *tanδ* decreased with increased cross-linker concentration, indicating that the toughness of obtained PAM–CNC hydrogel with high cross-linker concentration was weakened even though its strength improved significantly.

Influence of polymerization temperature for PAM–CNC hydrogels

It is well known that temperature was an important effect on the free-radical polymerization process with chemical initiator because the initiator dissociation rate depends on temperature (i.e., the higher the temperature, the higher the initiator dissociation rate) [29]. In addition, the temperature also influences the reactivity of the different molecules existed in solution during the propagation and termination stages. In order to investigate the effect of CNCs during polymerization, the G' and *tanδ* as a function of time were determined for PAM–CNC hydrogel system at 5, 25, 35, and 45 °C of polymerization temperature, and the result is shown in Fig. 5.

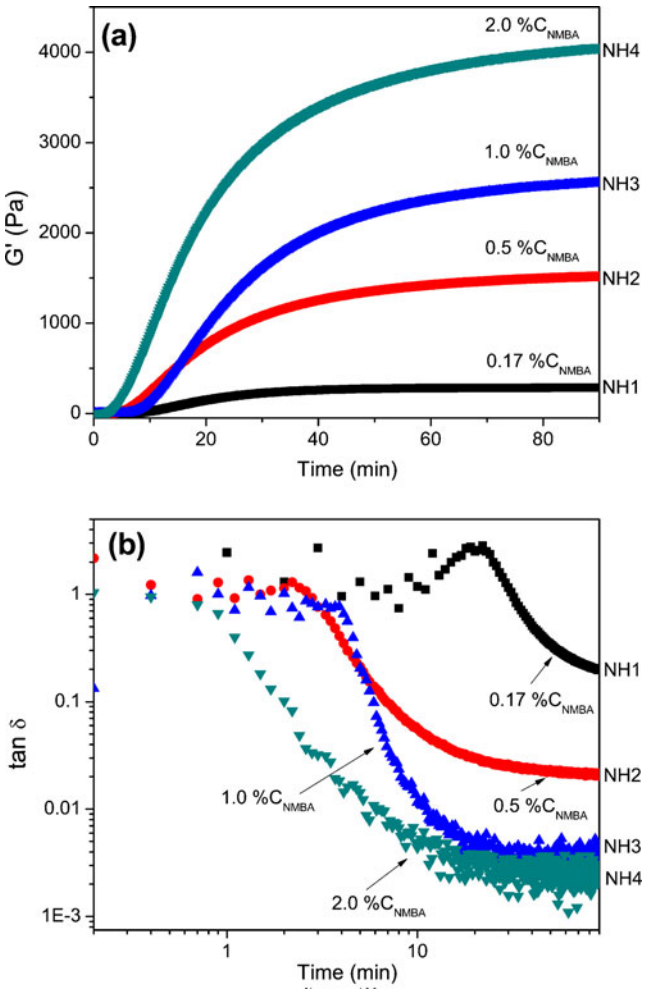

Fig. 4 Variations of elastic modulus G' (**a**) and loss factor *tanδ* (**b**) of PAM–CNC nanocomposite hydrogels as a function of polymerization time for different cross-linker concentrations

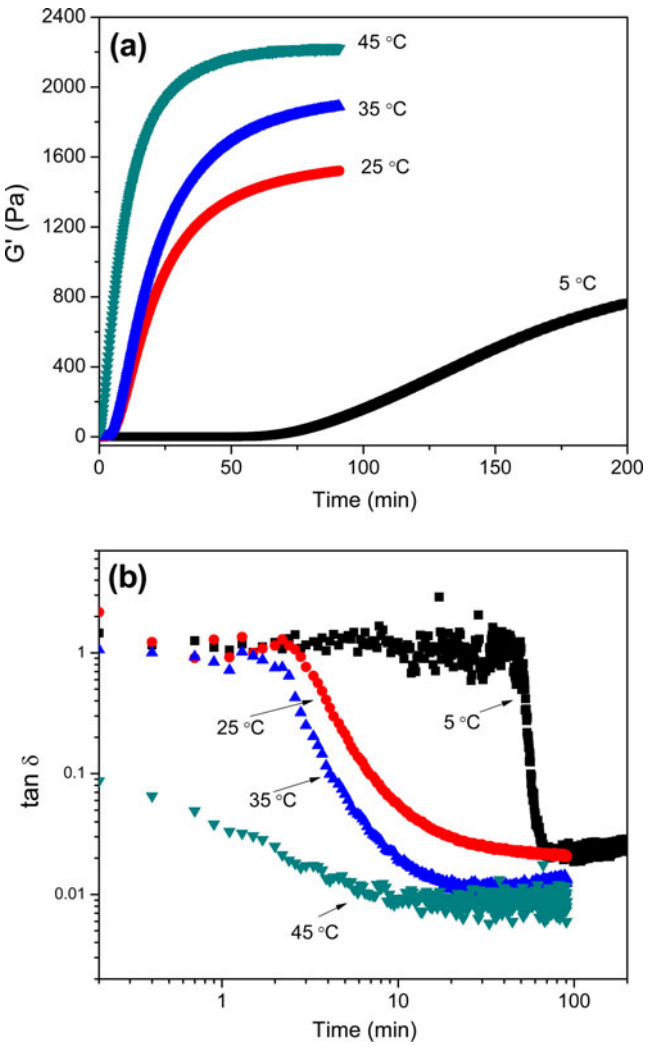

Fig. 5 Variations of elastic modulus G' (**a**) and loss factor *tanδ* (**b**) of PAM–CNC nanocomposite hydrogels as a function of polymerization time at various polymerization temperatures

From Fig. 4a, the values of G'_{∞} increased with polymerization temperature and reached a plateau value. The increase in G'_{∞} for PAM–CNC hydrogel with 0.5 wt% of cross-linkers reached about 220% from 5 to 45 °C, which is similar to the value of PAM hydrogel with 5.66 wt% of cross-linkers reported by Calvet et al. [14]. This result indicates that CNC did act as a multifunction cross-linker to improve the strength of hydrogel. The increase of the asymptotic slope at the half-gelation time P indicated that the sol–gel transition kinetics increased with temperature. In addition, it can be seen that N increased as increase of temperature for a constant AM and CNCs, which is similar to pure PAM hydrogen system. It is evident that temperature promoted the gelation process and shortened connecting chains between two junctions. The t_{onset} decreased with increased temperature, showing that the gelation point appeared more quickly at higher temperatures. t_{onset} was 51.8±4.5 min at 5 °C, suggesting the fact that the low temperature could effectively restrain the gelation process of PAM–CNC hydrogel. The t_{onset} closed to 0 min for 45 °C exhibited the high temperature improved the formation of microgels in PAM–CNC system. It is noted that t_{onset} = 0 did not indicate the inexistence of gelation point for PAM–CNC and yet indicated that the critical exponent of $tan\delta$=1 sometimes was not universal at the detection of gelation point for the rapid forming PAM–CNC network [30]. The decreased plateau $tan\delta$ with increased polymerization temperature showed that the high temperature reduced the toughness of hydrogels.

Effect of initiator concentration for PAM–CNC hydrogels

In considering the fact that polymer molecular weight (M_w) depended strongly on the initiator concentration for PAM

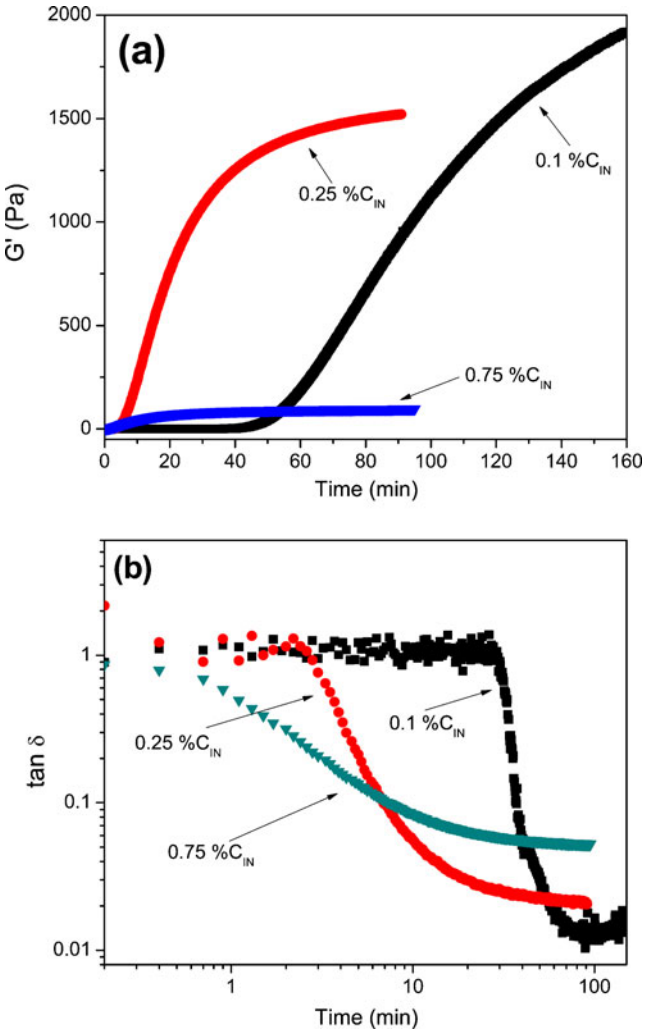

Fig. 6 Variations of elastic modulus G' (**a**) and loss factor $tan\delta$ (**b**) of PAM–CNC nanocomposite hydrogels as a function of polymerization time for different initiator concentrations

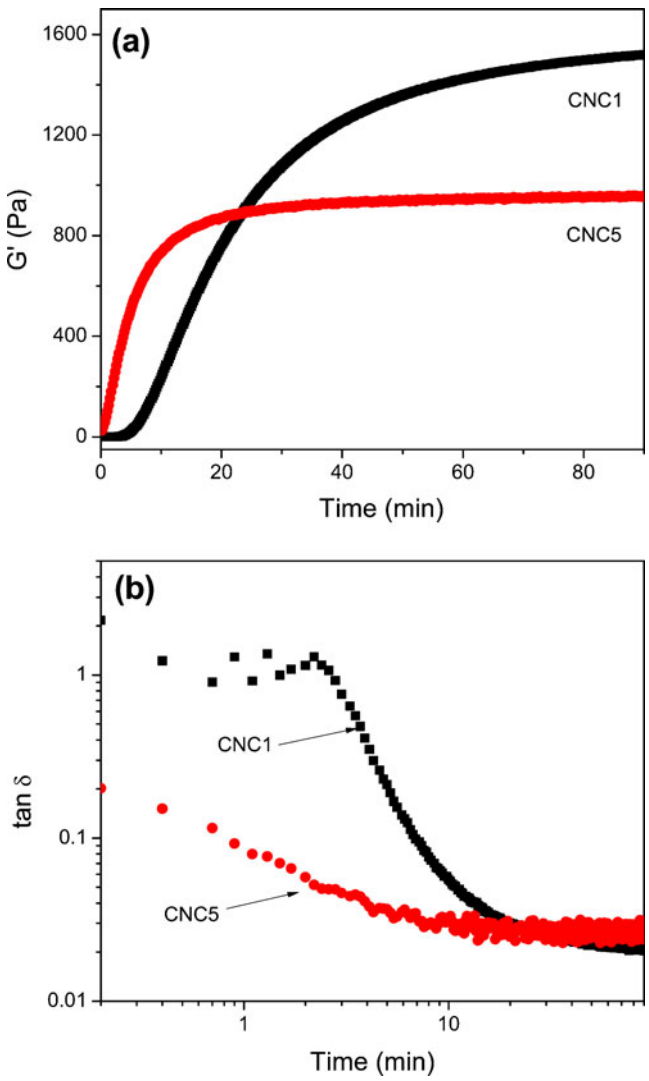

Fig. 7 Variations of elastic modulus G' (**a**) and loss factor $tan\delta$ (**b**) of PAM–CNC nanocomposite hydrogels as a function of polymerization time for two different CNC dimensions

polymerization [29], the gelation process of PAM–CNC system with different initiator concentration was investigated. Figure 5 shows the G' and $tan\delta$ as a function of time for PAM–CNC hydrogels with 0.1, 0.25, and 0.75 wt% of initiator concentration. For the induction stage, t_{onset} increased with the increase of initiator concentration because more radicals obtained in high initiator concentration accelerated the formation of chemical and physical network for the PAM–CNC system. For the sol–gel transition stage, the maximum value of P (41.4 ± 2.5 Pa min^{-1}) was obtained for 0.25 wt% of initiator concentration at 25 °C, suggesting the fact that the sol–gel process of PAM–CNC hydrogels reached optimization with 0.25 wt% of the initiator concentration. After the gelation was completed, the value of G'_{∞} decreased as the increased initiator concentration, which showed that the strength of obtained PAM–CNC hydrogel reduced under high initiator concentration. This behavior was attributed to the fact that M_w was inversely proportional to the initiator concentration for PAM polymerization, resulting in increasing initiator concentration that shortens or even breaks the connecting polymer chains between two junctions (a sketch is shown in Fig. 3b) [31]. Hence, the effective network junction was reduced, which confirmed by the change of N. From Fig. 6b, it also can be seen that the plateau $tan\delta$ decreased with increased initiator concentration.

Effect of CNC dimension for PAM–CNC hydrogels

Figure 7 shows the variation of the G' and $tan\delta$ with time for the PAM–CNC system including different aspect ratios of CNCs. It is noted that the decreased aspect ratios of CNCs improved P and t_{onset}, suggesting that CNCs with lower dimension promoted the formation of network likely because it absorbed more initiator and then formed more junction points resulting from its higher relative surface area and surface charge (as presented about zeta potential above). However, with the decrease of CNC dimension, G'_{∞} decreased, while plateau $tan\delta$ increased. This character is similar to that of initiator concentration and can be interpreted by the fact that the shortened rigid-rod cellulose nanocrystals reduced the effective network junction because it also acted as multifunctional cross-linker through the chemical bonding and physical adsorption with PAM network. Decreased effective network junction was verified with the change of N. A simple scheme is shown in Fig. 3c.

Conclusion

A series of in situ rheology experiments for the gelation process of PAM–CNC nanocomposite hydrogels were performed to investigate the influence of chemical cross-linker concentration, polymerization temperature, initiator concentration, and CNC aspect ratios on the elastic modulus (G') and loss factor ($tan\delta$). The investigation on the gelation reaction of PAM–CNC hydrogels demonstrated the fact that CNCs accelerated the onset of gelation (t_{onset}) and acted as a multifunctional cross-linker for the network of gels. The nanocomposite hydrogels with 5 wt% of CNC concentration exhibited an enhancement in both steady-state elastic modulus $\left(G'_{\infty}\right)$ and plateau $tan\delta$ compared to the pure PAM hydrogels, indicating that adding CNCs not only reinforced but also toughened PAM hydrogels. G'_{∞} and the effective network junction density (N) increased with increased cross-linker concentration, polymerization temperature, and CNC aspect ratios, and decreased with increased initiator concentration. The changes of plateau $tan\delta$ were opposite to that of G'_{∞}. t_{onset} decreased with increased cross-linker concentration, polymerization temperature, and initiator concentration. The sol–gel transition kinetics of PAM–CNC hydrogels were accelerated by increased cross-linker concentration and polymerization temperature, while reached optimization at 0.25 wt% of initiator concentration. CNCs with lower aspect ratios not only reduced t_{onset} but also promoted the sol–gel transition of PAM–CNC hydrogels, suggesting the fact that CNCs with the higher relative surface and surface charge had the ability to facilitate the formation of network. Thus, dynamic rheology technique offered a facile and powerful approach to characterize in situ polymerization process of nanocomposite hydrogels and to explore the forming mechanism of gelation.

Acknowledgments We thank the financial support from Louisiana Board of Regents Industrial Tie Subprogram (LEQSF(2010-13)-RD-B-01).

References

1. Schexnailder P, Schmidt G (2009) Nanocomposite polymer hydrogels. Colloid Polym Sci 287(1):1–11. doi:10.1007/s00396-008-1949-0
2. Samantha A, Meenach KWA, Zach Hilt J (2009) Hydrogel nanocomposites: Biomedical applications, biocompatibility, and toxicity analysis. Safety of nanoparticles from manufacturing to medical applications. Springer, New York
3. Lin DC, Yurke B, Langrana NA (2004) Mechanical properties of a reversible, DNA-crosslinked polyacrylamide hydrogel. J Biomech Eng-Transactions of the Asme 126(1):104–110. doi:10.1115/1.1645529
4. Hynd MR, Turner JN, Shain W (2007) Applications of hydrogels for neural cell engineering. J Biomater Sci Polym Ed 18 (10):1223–1244
5. Zhang JT, Huang SW, Xue YN, Zhuo RX (2005) Poly(n-isopropylacrylamide) nanoparticle-incorporated pnipaam hydrogels with fast shrinking kinetics. Macromol Rapid Commun 26 (16):1346–1350. doi:10.1002/marc.200500298

6. Wu YT, Zhou Z, Fan QQ, Chen L, Zhu MF (2009) Facile in-situ fabrication of novel organic nanoparticle hydrogels with excellent mechanical properties. J Mater Chem 19(39):7340–7346. doi:10.1039/B909125d
7. Hou Y, Matthews AR, Smitherman AM, Bulick AS, Hahn MS, Hou H, Han A, Grunlan MA (2008) Thermoresponsive nanocomposite hydrogels with cell-releasing behavior. Biomaterials 29 (22):3175–3184. doi:10.1016/j.biomaterials.2008.04.024
8. Zhu MF, Liu Y, Sun B, Zhang W, Liu XL, Yu H, Zhang Y, Kuckling D, Adler HJP (2006) A novel highly resilient nanocomposite hydrogel with low hysteresis and ultrahigh elongation. Macromol Rapid Commun 27(13):1023–1028. doi:10.1002/marc.200600159
9. Haraguchi K, Takehisa T (2002) Nanocomposite hydrogels: A unique organic-inorganic network structure with extraordinary mechanical, optical, and swelling/de-swelling properties. Adv Mater 14(16):1120–1124
10. Saravanan P, Raju MP, Alam S (2007) A study on synthesis and properties of ag nanoparticles immobilized polyacrylamide hydrogel composites. Mater Chem Phys 103(2–3):278–282. doi:10.1016/j.matchemphys.2007.02.025
11. Zhou C, Wu Q, Yue Y, Zhang Q (2011) Application of rod-shaped cellulose nanocrystals in polyacrylamide hydrogels. J Colloid Interface Sci 353(1):116–123. doi:10.1016/j.jcis.2010.09.035
12. Tang YF, Du YM, Hu XW, Shi XW, Kennedy JF (2007) Rheological characterisation of a novel thermosensitive chitosan/poly(vinyl alcohol) blend hydrogel. Carbohydr Polym 67(4):491–499. doi:10.1016/j.carbpol.2006.06.015
13. Wang J, Ugaz VM (2006) Using in situ rheology to characterize the microstructure in photopolymerized polyacrylarnide gels for DNA electrophoresis. Electrophoresis 27(17):3349–3358. doi:10.1002/elps.200500910
14. Calvet D, Wong JY, Giasson S (2004) Rheological monitoring of polyacrylamide gelation: Importance of cross-link density and temperature. Macromolecules 37(20):7762–7771. doi:10.1021/Ma049072r
15. Nita LE, Chiriac AP, Bercea M, Neamtu I (2007) In situ monitoring the sol-gel transition for polyacrylamide gel. Rheologica Acta 46(5):595–600. doi:10.1007/s00397-006-0141-z
16. Neamtu I, Nita LE, Chiriac AP, Bercea M (2006) Rheological monitoring of in situ poly(acrylamide) gel preparation. J Optoelectron Adv Mater 8(1):201–204
17. Okay O, Oppermann W (2007) Polyacrylamide-clay nanocomposite hydrogels: Rheological and light scattering characterization. Macromolecules 40(9):3378–3387. doi:10.1021/Ma062929v
18. Aalaie J, Vasheghani-Farahani E, Rahmatpour A, Semsarzadeh MA (2008) Effect of montmorillonite on gelation and swelling behavior of sulfonated polyacrylamide nanocomposite hydrogels in electrolyte solutions. Eur Polym J 44(7):2024–2031. doi:10.1016/j.eurpolymj.2008.04.031
19. Liu H, Liu D, Yao F, Wu Q (2010) Fabrication and properties of transparent polymethylmethacrylate/cellulose nanocrystal composites. Bioresour Technol 101(14):5685–5692
20. Zhou C, Yang W, Yu Z, Zhou W, Xia Y, Han Z, Wu Q (2010) Synthesis and solution properties of novel comb-shaped acrylamide copolymers. Polymer Bulletin:Online. doi:10.1007/s00289-010-0360-4
21. Bercea M, Navard P (2000) Shear dynamics of aqueous suspensions of cellulose whiskers. Macromolecules 33(16):6011–6016
22. Peresin MS, Habibi Y, Zoppe JO, Pawlak JJ, Rojas OJ (2010) Nanofiber composites of polyvinyl alcohol and cellulose nanocrystals: Manufacture and characterization. Biomacromolecules 11 (3):674–681. doi:10.1021/Bm901254n
23. Lu P, Hsieh Y-L (2010) Preparation and properties of cellulose nanocrystals: Rods, spheres, and network. Carbohydr Polym 82 (2):329–336. doi:10.1016/j.carbpol.2010.04.073
24. Agoda-Tandjawa G, Durand S, Berot S, Blassel C, Gaillard C, Garnier C, Doublier JL (2010) Rheological characterization of microfibrillated cellulose suspensions after freezing. Carbohydr Polym 80(3):677–686. doi:10.1016/j.carbpol.2009.11.045
25. Haraguchi K, Li HJ, Matsuda K, Takehisa T, Elliott E (2005) Mechanism of forming organic/inorganic network structures during in-situ free-radical polymerization in pnipa-clay nanocomposite hydrogels. Macromolecules 38(8):3482–3490. doi:10.1021/Ma047431c
26. Xiong LJ, Hu XB, Liu XX, Tong Z (2008) Network chain density and relaxation of in situ synthesized polyacrylamide/hectorite clay nanocomposite hydrogels with ultrahigh tensibility. Polymer 49 (23):5064–5071. doi:10.1016/j.polymer.2008.09.021
27. Abdurrahmanoglu S, Can V, Okay O (2009) Design of high-toughness polyacrylamide hydrogels by hydrophobic modification. Polymer 50(23):5449–5455. doi:10.1016/j.polymer.2009.09.042
28. Orakdogen N, Okay O (2006) Correlation between crosslinking efficiency and spatial inhomogeneity in poly(acrylamide) hydrogels. Polym Bull 57(5):631–641. doi:10.1007/s00289-006-0624-1
29. Giz A, Catalgil-Giz H, Alb A, Brousseau JL, Reed WF (2001) Kinetics and mechanisms of acrylamide polymerization from absolute, online monitoring of polymerization reaction. Macromolecules 34(5):1180–1191. doi:10.1021/Ma000815s
30. Harini M, Deshpande AP (2009) Rheology of poly(sodium acrylate) hydrogels during cross-linking with and without cellulose microfibrils. J Rheol 53(1):31–47. doi:10.1122/1.3003054
31. Lin HR (2001) Solution polymerization of acrylamide using potassium persulfate as an initiator: Kinetic studies, temperature and ph dependence. Eur Polym J 37(7):1507–1510